

Fragment Production in Non-central Collisions of Intermediate Energy Heavy Ions

B. Davin, R. Alfaro, H. Xu, L. Beaulieu,* Y. Larochelle,* T. Lefort,† R. Yanez,‡ S. Hudan, A.L. Caraley, and R.T. de Souza
*Department of Chemistry and Indiana University Cyclotron Facility,
Indiana University, Bloomington, IN 47405*

T.X. Liu, X.D. Liu, W.G. Lynch, R. Shomin, W.P. Tan, M.B. Tsang, A. Vander Molen, A. Wagner,§ H.F. Xi, and C.K. Gelbke
*National Superconducting Cyclotron Laboratory and Department of Physics and Astronomy,
Michigan State University, East Lansing, MI 48824*

R.J. Charity and L.G. Sobotka
Department of Chemistry, Washington University, St. Louis, MO 63130
(Dated: November 1, 2018)

The defining characteristics of fragment emission resulting from the non-central collision of ^{114}Cd ions with ^{92}Mo target nuclei at $E/A = 50$ MeV are presented. Charge correlations and average relative velocities for mid-velocity fragment emission exhibit significant differences when compared to standard statistical decay. These differences associated with similar velocity dissipation are indicative of the influence of the entrance channel dynamics on the fragment production process.

PACS numbers: PACS number(s): 25.70.Mn

Peripheral and mid-central collisions of two heavy-ions at intermediate energies ($20 \text{ MeV} \leq E/A \leq 50 \text{ MeV}$) result in the copious production of intermediate mass fragments (IMF: $3 \leq Z \leq 20$). Whether these fragments originate from the surface instability of non-spherical, transient geometries produced in nucleus-nucleus collisions [1, 2] or arise from proximity-enhanced, statistical decay of the projectile-like and target-like fragments [3] remains an open question. Fragment production as a result of dynamical surface instabilities would provide insight into the fragmentation mechanism of deformed nuclear matter at modest excitation energies. Alternatively, observation of the statistical decay of nuclear matter in the presence of an external long-range force represents a new and unexplored domain.

At low incident energies, $E/A \leq 10$ MeV, nucleon transport between two colliding nuclei is Pauli-blocked, allowing the projectile and target nuclei to remain approximately intact. Nucleons are exchanged *via* the “neck” (overlap region) connecting the two nuclei by a largely stochastic process [4]. Occasionally, dynamical neck rupture driven by surface instabilities can lead to production of fragments between the two reaction partners [1]. In contrast, at high incident energies, $E/A \geq 100$ MeV, where nucleon-nucleon collisions dominate, the “participant” region of overlap between the two nuclei becomes highly excited and rapidly disintegrates into a broad spectrum

of nucleons and light nuclei [5, 6]. In this work, we are concerned with the origin of fragments at intermediate energies, $E/A = 20\text{-}50$ MeV, where experiments have observed copious IMF yields at velocities between the projectile-like and target-like residues [2, 7, 8, 9, 10, 11]. Since emission of such fragments is a robust prediction of transport theories [12], these “neck fragments” are often regarded as dynamical in origin [13]. Recent theoretical and experimental analyses [3, 14] however, have considered the statistical origin of such fragments. Thus, it is important to determine the defining characteristics associated with these fragments in order to elucidate the relevant mechanism.

To explore the issues outlined above, we have examined peripheral and mid-central collisions in which interaction of projectile and target nuclei results in the production of an excited projectile-like fragment (PLF*) that can decay either by evaporation or fission. If the creation of the PLF* and its subsequent decay are sufficiently decoupled, one expects the decay of the PLF* to be isotropic in its own rest frame. Alternatively, coupling between the formation of the PLF* and its decay could result in an anisotropic decay pattern. Additionally, even if the formation and decay of the PLF* are decoupled, dynamical breakup, (*e.g.* neck rupture [1, 15]) or the proximity influence of the target-like fragment (TLF) may result in different characteristics (*e.g.* yield, relative velocities) of fragments emitted forward and backward of the PLF*.

The experiment was performed at the National Superconducting Cyclotron Laboratory at Michigan State University where a beam of ^{114}Cd ions, accelerated by the K1200 cyclotron to $E/A = 50$ MeV, bombarded a 5.45 mg/cm^2 thick ^{92}Mo target foil. Charged reaction products were detected by a setup which subtended 80% of 4π . In the range $2.1^\circ \leq \theta_{lab} \leq 4.2^\circ$, forward moving charged

*Present address: Universite Laval, Quebec, Canada.

†Present address: Universite de Caen, Caen, France.

‡Present address: Universidad de Chile, Santiago, Chile.

§Present address: Institute of Nuclear and Hadron Physics, Forschungszentrum, Rossendorf, Dresden, Germany.

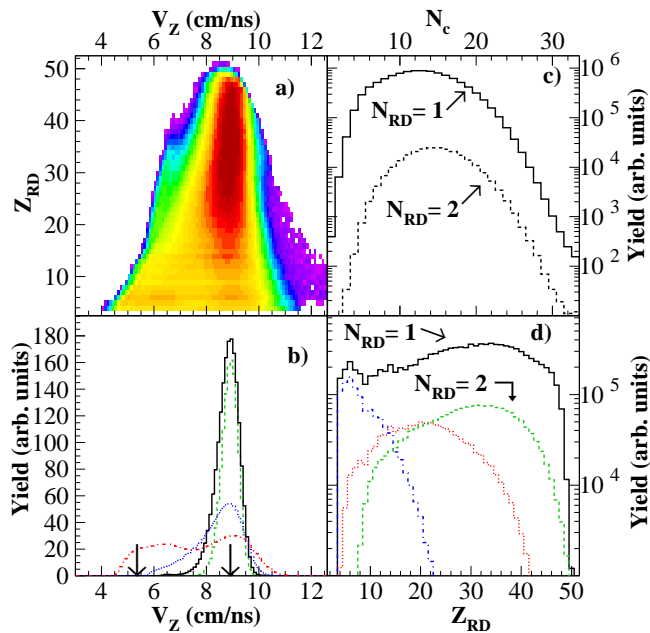


FIG. 1: a) Z_{RD} vs. velocity for fragments detected in the ring detector (RD) associated with $N_c \geq 3$. b) Fragment v_Z distributions in the RD for different intervals in Z ($40 \leq Z \leq 45$ (dashed, green), $30 \leq Z \leq 35$ (solid, black), $15 \leq Z \leq 20$ (dotted, blue), or $4 \leq Z \leq 10$ (dot-dash, red)). Arrows depict the center-of-mass velocity (left) and beam velocity (right). c) Multiplicity distributions associated with $N_{RD} = 1$ (solid) and $N_{RD} = 2$ (dashed). d) Z distribution of fragments measured in the RD when $N_{RD} = 1$ (solid, black) and $N_{RD} = 2$ (dashed, green) and for the two fragments individually (dots, red, larger fragment; dot-dash, blue, smaller fragment).

products were detected by a 300 μm thick, segmented silicon ring counter (RC). The RC had 4 separate quadrants of 16 independent annular sections on its front face and 16 pie-shaped sectors on its back face and was thus capable of identifying multiple charged particles. Behind each pie-sector, and covering the same solid angle, was a 2-cm thick CsI(Tl) crystal read-out with a photodiode. Identification thresholds in the RC detector (RD) ranged from ≈ 9 MeV/A for Be to ≈ 25 MeV/A for Cd, with better than unit Z resolution for $Z \leq 48$. Fragment velocities were determined by assigning the A from the measured Z using the systematics of Ref. [16]. Reaction products emitted at larger angles ($7^\circ \leq \theta_{lab} \leq 168^\circ$) were detected by the silicon strip array LASSA [17], and the Miniball-Miniwall 4π array [18].

Some general features of the reaction are depicted in Fig. 1. Events were selected by the requirement that at least three charged particles were detected in the Miniball/Miniwall array and at least one charged particle was detected in the RD. The relationship between the charge and velocity of the detected fragments in the RD is depicted in Fig. 1a. One observes a vertical ridge of fragments centered at approximately 9.0 cm/ns that in-

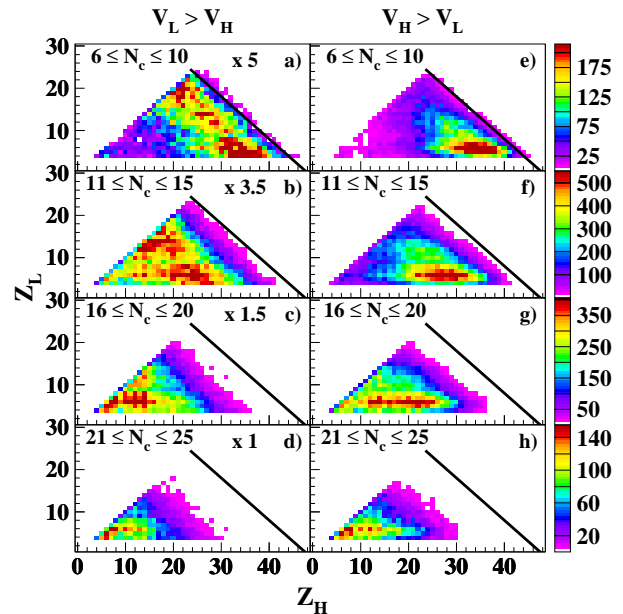


FIG. 2: Charge correlation between the two fragments detected in the RD selected on both the magnitudes of the fragment velocities and N_c .

creases in width as Z decreases. In Fig. 1b, velocity distributions are displayed for fragments detected in the RD and selected on different intervals in Z . When the fragment detected in the RD is large, $40 \leq Z \leq 45$ (dashed, green), $30 \leq Z \leq 35$ (solid, black), or $15 \leq Z \leq 20$ (dotted, blue), the velocity distribution is peaked at ≈ 8.95 cm/ns. This constancy in the velocity of the PLF has been attributed to decoupling of the overlap region from the non-overlap region (participant-spectator scenario) [19]. However, for the smallest fragments detected in the RD, $4 \leq Z \leq 10$ (dot-dash, red), the distribution of velocities is bimodal, with peaks at velocities of ≈ 6.4 and ≈ 9.1 cm/ns.

In order to study the decay properties of the PLF* produced in the peripheral and mid-central collisions we examine events in which two fragments ($Z \geq 4$) are detected in the RD. The high angular granularity of the RD allows us to selectively study the binary decay of the PLF* along its flight direction. This selection has been shown to be a sensitive probe of the decay characteristics of the PLF* [20]. To begin we compare the charged particle multiplicity, N_c , distributions associated with detection of one ($N_{RD}=1$) or two ($N_{RD}=2$) fragments in the RD as shown in Fig. 1c. When $N_{RD}=1$, $\langle N_c \rangle = 12.5$ with a FWHM of 5.0. The multiplicity distribution associated with $N_{RD}=2$, does not differ substantially and has a mean value and FWHM of 14.8 and 4.0 respectively. On the basis of N_c alone, these two cases appear similar.

The Z distributions of fragments in the ring detector, Z_{RD} , corresponding to $N_{RD}=1$ and $N_{RD}=2$, are shown in Fig. 1d. When $N_{RD}=1$, the Z distribution is broad and peaked at $Z_{RD} \approx 32$. When $N_{RD}=2$, the dis-

tribution of total charge in the RD (dashed histogram, green) is similar to $N_{RD}=1$ (solid, black). The individual Z distributions for the larger fragment (dot, red) and smaller fragment (dot-dash, blue) are displayed for reference. The similarity of the total charge distribution when $N_{RD}=2$, to the Z distribution for $N_{RD}=1$ suggests that these events do not differ significantly from the $N_{RD}=1$ case.

We have further separated the events with $N_{RD}=2$ into two groups based upon the magnitudes of the fragment velocities. In the first group, the smaller fragment is faster ($v_L > v_H$), while in the second group the larger fragment is faster ($v_H > v_L$). If the decay of the PLF* is decoupled from its formation, and the decay is statistical, the characteristics of these two groups of events should be identical.

The charge correlation between the two fragments detected in the RD is depicted in Fig. 2 as a function of N_c . In the left-hand column, the charge correlation between the two fragments for events in which $v_L > v_H$ is shown. For the lowest multiplicity interval (Fig. 2a) a ridge of anti-correlated yield is observed – consistent with the binary decay of a single parent fragment. For reference, the solid line corresponding to $Z_H + Z_L = 48$ is displayed. The shift of the ridge from this line indicates that the Z of the parent fragment, PLF*, is on average slightly smaller ($Z_H + Z_L \approx 41$) than the projectile atomic number. For the next multiplicity interval (Fig. 2b) a similar pattern is observed. The ridge of maximum yield has shifted to a smaller value ($Z_H + Z_L \approx 32$). This result is consistent with a less peripheral collision in an ablation/abrasion scenario or multi-particle emission from the PLF* before it splits into two fragments. We hypothesize that the observed binary pattern is fission-like in nature based upon lower energy investigation of angular correlations of similar systems [21, 22]. For higher multiplicities, the anti-correlation pattern is no longer clearly evident. The pattern for events in which $v_H > v_L$, is shown in the right-hand column of Fig. 2. For all the multiplicity intervals displayed (panels e - h), super-imposed on a broad anti-correlated band, a horizontal ridge is discernible.

The charge correlation patterns shown in Fig. 2 suggest a different behavior when $v_H > v_L$ as compared to $v_L > v_H$, the first evidence we are selecting two different mechanisms. When $v_H > v_L$, the horizontal ridge indicates that the size of the smaller fragment is largely independent of the size of the larger fragment and has a most probable value of $Z_L \approx 6$. We conclude this insensitivity of the magnitude Z_L to the magnitude of Z_H is a defining feature of this process. Such behavior is consistent with the smaller fragment arising from the dynamical breakup of a neck-like structure where the most probable size of the smaller fragment is determined by the diameter of a cylindrical neck [2], or from sufficiently different statistical emission conditions as compared to the case when $v_L > v_H$. It is interesting to note that for the multiplicity interval $6 \leq N_c \leq 10$, $\langle Z_L \rangle + \langle Z_H \rangle$ is essentially the same 37.6 and 38.3 for $v_L > v_H$ and $v_H > v_L$ respectively. This

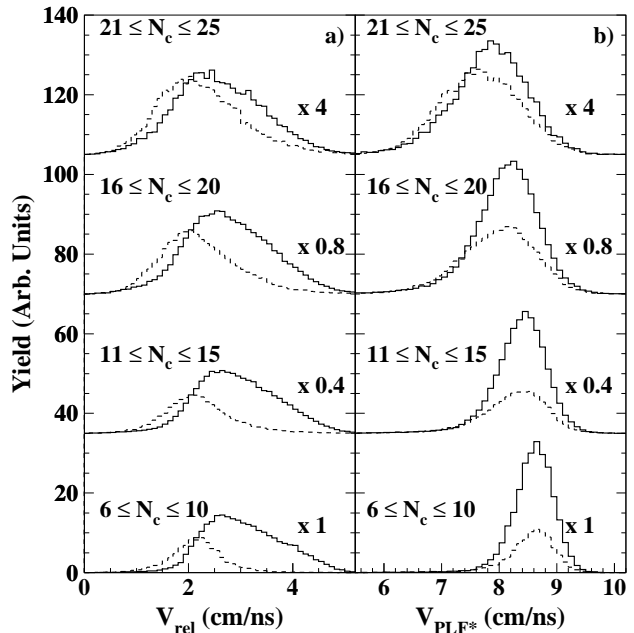


FIG. 3: a) Distributions of relative velocity between the two RD fragments for $v_H > v_L$ (solid histogram) and $v_L > v_H$ (dashed histogram) for the indicated selections on the charged particle multiplicity, N_c . b) Distributions of v_{PLF^*} , the center-of-mass velocity of the two fragments detected in the RD. Solid histograms represent the case for $v_H > v_L$ and dashed histogram the case $v_L > v_H$.

result is consistent with the N_c selection determining the impact parameter and hence the size of the fragmenting system in both cases. The difference between these *charge correlation patterns* observed for the two cases represents a distinguishing feature of the mid-velocity fragment emission not realized in earlier work [2, 20].

We have further examined the differences between the $v_H > v_L$ and $v_L > v_H$ cases by comparing the distributions of the relative velocity between these two fragments, $\vec{v}_{rel} = \vec{v}_H - \vec{v}_L$ and the distributions of their center-of-mass velocity, v_{PLF^*} , for selected cuts on the charged particle multiplicity, N_c . Evident in Fig. 3a is the fact that the v_{rel} distribution is broader with a higher mean value when $v_H > v_L$ as compared to $v_L > v_H$. This difference is largest when $6 \leq N_c \leq 10$. In contrast to the differences observed in v_{rel} , the distributions in v_{PLF^*} (Fig. 3b) for both cases are remarkably similar in both their average value and their width. Two trends are evident in Fig. 3b. With increasing N_c , the mean value of v_{PLF^*} decreases, and the width of the v_{PLF^*} distribution also increases systematically. If one relates the v_{PLF^*} to the velocity damping of the PLF and consequently its excitation, the trend of a decrease in the mean value of v_{PLF^*} with increasing N_c is reasonable.

The angular distribution between v_{rel} and v_{PLF^*} is examined in Fig. 4 for $6 \leq N_c \leq 25$ as a function of v_{rel} . We define $\cos(\alpha) = (\vec{v}_{PLF^*} \cdot \vec{v}_{rel}) / (v_{PLF^*} v_{rel})$. These two

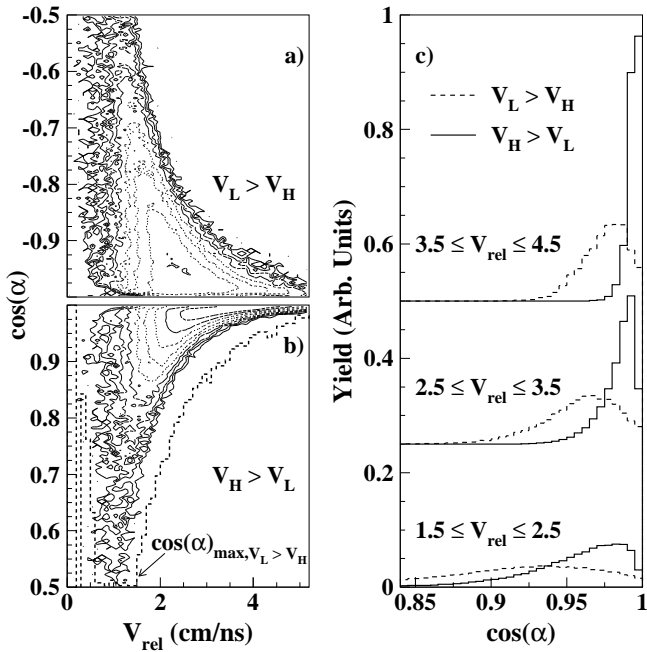


FIG. 4: Angular correlation between v_{rel} and v_{PLF^*} for $v_L > v_H$ (panel a) and $v_H > v_L$ (panel b). The dashed line in panel b) depicts the detector acceptance for the $v_L > v_H$ case. Angular distributions for $v_H > v_L$ (solid histogram) and $v_L > v_H$ (dashed histogram) for different intervals in v_{rel} are shown in panel c).

distributions are quantitatively different. When $v_H > v_L$ (Fig. 4b), the $\cos(\alpha)$ distribution is narrower than when $v_L > v_H$ (Fig. 4a). These two-dimensional distributions reflect both the true angular distribution and the influence of the detector acceptance. Depicted as a dashed line in panel b is the maximum value of $\cos(\alpha)$ for $v_L > v_H$ which we designate $\cos(\alpha)_{max, v_L > v_H}$, as a function of v_{rel} . The fact that the entire measured distribution for $v_H > v_L$ is less than $\cos(\alpha)_{max, v_L > v_H}$, suggests that the limited angular coverage of the RD *does not* present a significant problem for the $v_H > v_L$ case. Since the geometric acceptance depends on v_{PLF^*} , we have examined these same distributions for more restrictive conditions by selecting on $6 \leq N_c \leq 10$ so as to select a more defined v_{PLF^*} . The result of this more restrictive analysis supports the conclusion that for $v_H > v_L$ the experimental angular coverage is sufficient.

In order to more quantitatively compare the angular distributions between the two velocity cases, we show in Fig. 4c distributions in $\cos(\alpha)$ for different intervals in v_{rel} . Solid histograms represent the case $v_H > v_L$ and dashed histograms the case $v_L > v_H$. For all three intervals of v_{rel} shown, the distribution for $v_H > v_L$ is more sharply peaked towards $\cos(\alpha)=1$ than the $v_L > v_H$ distribution, indicating alignment of the two fragments is more probable when $v_H > v_L$. This observed angular correlation is consistent with the work of [20].

Based upon the charge correlations observed in Fig. 2,

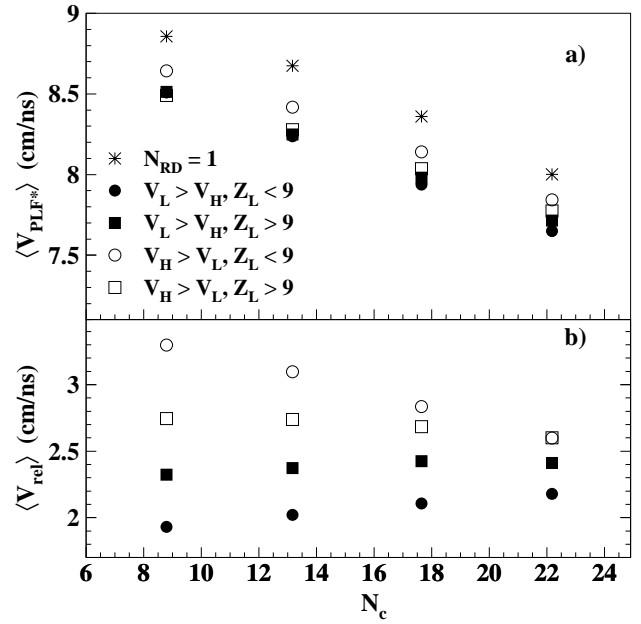


FIG. 5: a) Dependence of center-of-mass velocity of the two RD fragments on multiplicity. b) Relation between the relative velocity of the two fragments in the RD and N_c .

we have further subdivided both types of events according to the magnitude of Z_L : $Z_L < 9$ and $Z_L > 9$. The kinetic characteristics of the fragment pairs selected in this way are shown in Fig. 5. The average velocity of the PLF*, $\langle v_{PLF^*} \rangle$, is presented for the different cases in Fig. 5a. One observes that all four cases are clustered in a band, consistent with the behavior in Fig. 3b, with a lower velocity than the $N_{RD}=1$ case. The similar magnitude of $\langle v_{PLF^*} \rangle$ suggests that the velocity damping (excitation) of the system in all four cases is similar and larger than the velocity damping (excitation) in the $N_{RD}=1$ case. This conclusion is further borne out by examining the multiplicity of light charged particles detected. For the most peripheral collisions studied, *i.e.* the multiplicity interval $6 \leq N_c \leq 10$, $\langle N_H \rangle$ and $\langle N_{He} \rangle$ are 3.6 and 2.2 when $v_H > v_L$ and 3.6 and 2.3 when $v_L > v_H$. The similarity of the magnitude of v_{PLF^*} , for both velocity cases, as well as the similar light charged particle multiplicities suggests that the excitation (and spin) of the PLF* is essentially the same in both velocity cases.

We have also examined the dependence of the average relative velocity of the two fragments, $\langle v_{rel} \rangle$, on N_c as shown in Fig. 5b. For $v_L > v_H$ and $Z_L > 9$, (filled squares), $\langle v_{rel} \rangle$ is relatively constant as a function of N_c , suggesting that the decay of the PLF* is sufficiently decoupled from its formation. The average relative velocity increases slightly with N_c when $v_L > v_H$ and $Z_L < 9$, (filled circles). More symmetric splits ($Z_L > 9$) exhibit a somewhat larger $\langle v_{rel} \rangle$ (≈ 2.3 - 2.4 cm/ns) than more asymmetric ($Z_L < 9$) splits (≈ 1.9 - 2.2 cm/ns). Both these values of $\langle v_{rel} \rangle$ and the N_c independence are consistent with the

fission of a PLF* (Viola fission TKE systematics [23]) following an initial interaction which determines the N_c . When $v_H > v_L$ and $Z_L > 9$ (open squares) a similar independence of $\langle v_{rel} \rangle$ on N_c is observed although the magnitude of $\langle v_{rel} \rangle$ is slightly larger (≈ 2.6 - 2.8 cm/ns). This constancy of $\langle v_{rel} \rangle$ suggests that these events also arise from a mechanism similar to the two-stage fission-like behavior observed for $v_L > v_H$.

In marked contrast to the previously described fission-like behavior is the behavior for $Z_L < 9$ when $v_H > v_L$ (open circles). At low N_c for this case, $\langle v_{rel} \rangle$ is considerably higher than in the fission-like case. With increasing N_c (centrality) the $\langle v_{rel} \rangle$ for this case decreases. The monotonic decrease of $\langle v_{rel} \rangle$, in contrast to the near constant behavior observed for the other cases, suggests that in this case the fragment emission arises from a different mechanism – one coupled to formation of the PLF*. Large relative velocities have recently been reported [20] over a broad range of charge asymmetry for this additional component; however, the present work focuses on the most extreme asymmetries for which we determine the effect is the largest. Moreover, we determine, for the first time, that these large differences in $\langle v_{rel} \rangle$ are associated with essentially the same dissipation.

As the largest variations in $\langle v_{rel} \rangle$ are evident for $6 \leq N_c \leq 10$, we now focus on this multiplicity interval. Comparison of $\langle v_{rel} \rangle$ in Fig. 5 between $Z_L < 9$ and $Z_L > 9$ for either $v_L > v_H$ or $v_H > v_L$ suggests a dependence of $\langle v_{rel} \rangle$ on Z_L . In Fig. 6a, one observes that the two velocity cases manifest different trends of $\langle v_{rel} \rangle$ with increasing Z_L . For events selected with $v_L > v_H$ (closed circles), $\langle v_{rel} \rangle$ is approximately constant for $Z_L \geq 7$, consistent with the Viola fission systematics (solid line) [23], *i.e.* a Coulomb dominated separation. For $Z_L \leq 6$, the values of $\langle v_{rel} \rangle$ are somewhat lower than expected possibly due to reduced efficiency for triggering on fast, light fragments in the RD. In addition, the influence of secondary decay effects, increases in magnitude with decreasing Z_L . The error bars shown reflect the uncertainty due to the deduced mass of the fragment.

For the case of $v_H > v_L$ (open circles), one observes a significantly larger magnitude for $\langle v_{rel} \rangle$, which decreases as Z_L increases. The enhancement of relative velocity above the Coulomb lower limit (solid line) is approximately 40% for $Z=4$. We conclude this enhancement is another defining characteristic of mid-rapidity fragment emission. Correction for the finite acceptance and thresholds of the RD result in the open triangles displayed in Fig. 6. These restrictions do not change the qualitative description of the data and only result in enhancing the observed trends.

Insight into the mechanism of mid-rapidity fragment production is provided by considering the possible sources of the the observed enhancement in $\langle v_{rel} \rangle$. Fragments acquire their velocities from any of three possible sources: Coulomb repulsion, thermal energy, or collective motion. The difference in $\langle v_{rel} \rangle$ observed in Fig. 6a cannot be attributed to Coulomb repulsion, nor to sig-

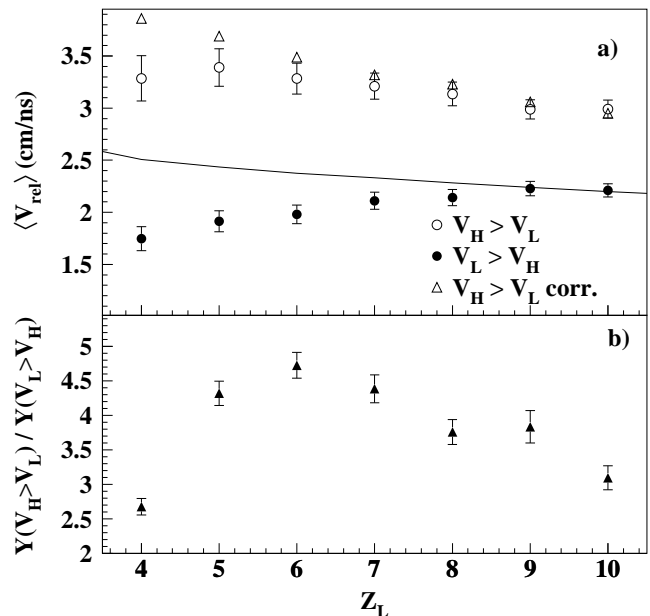


FIG. 6: a) Dependence of the relative velocity of the two fragments detected in the RD on the charge of the smaller fragment, Z_L . b) Ratio of the yield of Z_L for the two cases $v_H > v_L$ and $v_L > v_H$, when $6 \leq N_c \leq 10$.

nificant thermal differences due to the N_c selection (and supported by the average multiplicity of light charged particles). Thus, the significant enhancement of $\langle v_{rel} \rangle$ is most likely collective in origin and due to coupling to the considerable collective motion present in the entrance channel.

In Fig. 6b we present the ratio of the measured yields of $v_H > v_L$ to $v_L > v_H$ as a function of Z_L (closed triangles). Over the entire range of Z_L displayed, the yield for the $v_H > v_L$ case is larger than the $v_L > v_H$ case by a factor of 2.6-4.7 and reaches a maximum at $Z_L = 6$. This enhancement of yield at velocities intermediate between the PLF and TLF is comparable to the enhancement observed previously [2].

In order to characterize the nature of the coupling to the entrance channel, we examine the Z distribution for peripheral collisions ($6 \leq N_c \leq 10$) selected on the velocity of the PLF*. For this multiplicity interval the most probable value of $Z_H + Z_L$ is ≈ 41 in both cases. The velocity distribution of the PLF* for both $v_H > v_L$ and $v_L > v_H$ is approximately gaussian with $\langle v_{cm} \rangle = 8.6, 8.5$ cm/ns and a FWHM = 0.41, 0.50 cm/ns for $v_H > v_L$ and $v_L > v_H$, respectively. A decrease in v_{PLF^*} is related to an increase in the velocity dissipation and consequently an increase in the excitation of the PLF* and possibly a change in its spin. In Fig. 7 we examine the Z distribution selected on progressively decreasing values of v_{PLF^*} for both $v_L > v_H$ (solid symbols) and $v_H > v_L$ (open symbols). One observes that for the fission-like case, *i.e.* $v_L > v_H$ (closed symbols), for the case of the least dissipation $8.9 < v_{PLF^*} \text{ (cm/ns)} \leq 9.2$, the Z distribu-

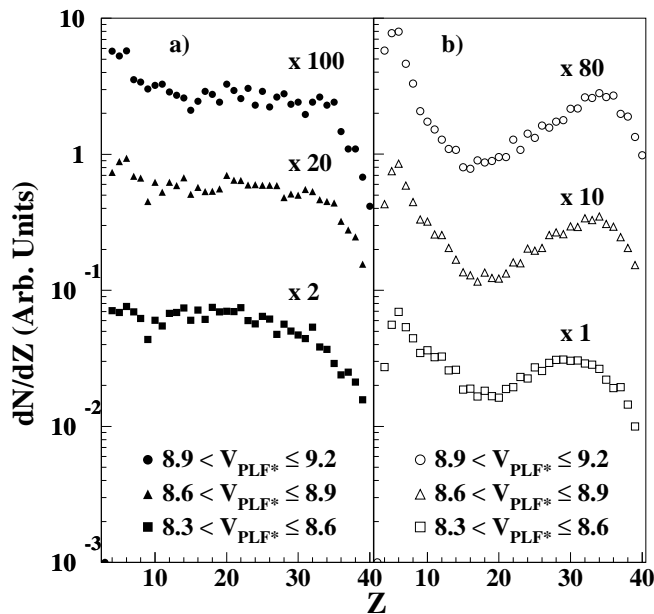


FIG. 7: Z distributions when $6 \leq N_c \leq 10$ for $8.9 < v_{PLF^*}$ (cm/ns) ≤ 9.2 , $8.6 < v_{PLF^*}$ (cm/ns) ≤ 8.9 , and $8.3 < v_{PLF^*}$ (cm/ns) ≤ 8.6 , when $v_L > v_H$ (solid symbols) and $v_H > v_L$ (open symbols).

tion is slightly asymmetric. With increasing dissipation the distribution becomes relatively flat. An asymmetric distribution can be understood in terms of the fissility of a light nucleus and the Businaro-Gallone point [20, 24]. As the transition from an asymmetric to a symmetric Z distribution is more sensitive to the spin of the decaying nucleus as compared to its excitation, it is likely that the transition observed for the fission-like case is due to increased spin of the PLF* as v_{PLF^*} decreases. For a light system, such as $Z=40$, with low spin one expects an asymmetric Z distribution; with increasing spin, approaching the critical angular momentum allowed for a rotating nucleus, a transition to an increasingly flat Z distribution is expected [24]. One can alternatively relate the asymmetric component of the Z distribution to evaporation and the symmetric component to fission. While excitation alone favors evaporation, inclusion of spin enhances the

importance of the fission channel. The transition from a slightly asymmetric distribution to a flat one with increasing velocity damping can be related to the relative importance of symmetric fission as compared to evaporation and consequently the excitation and spin of the decaying system.

In contrast to the behavior observed for the fission-like case, when $v_H > v_L$ (open symbols) the Z distribution is always asymmetric and maintains its asymmetry over the same interval in v_{PLF^*} during which the $v_L > v_H$ makes the transition from slightly asymmetric to flat. This behavior of the Z distribution asymmetry when $v_H > v_L$ suggests that the breakup in this case is driven by factors other than excitation or spin. The observation of dynamically driven fragment production in *hot* ternary fission [25] may indicate a common origin of mid-velocity fragments.

In summary, examination of fragment emission forward and backward of an excited projectile-like fragment formed in the peripheral or mid-central collision of two heavy-ions reveals two types of decay processes. One process is consistent with the standard statistical fission-like decay while the other, associated with mid-velocity fragment emission, clearly reflects the influence of the entrance channel, hence is a dynamical process. These two processes exhibit *substantially different charge correlations*. Focusing on the most peripheral collisions, we have further compared these two decay modes on the basis of the dissipated velocity and we find that *for essentially the same velocity dissipation the $\langle v_{rel} \rangle$ and the Z distributions differ markedly*. Neither excitation nor spin of the PLF* can explain either the asymmetry of the Z distribution for the dynamical component or the persistence of this asymmetry with increased velocity damping.

We would like to thank the staff at MSU-NSCL for providing the high quality beams which made this experiment possible. One of the authors (RdS) is grateful to Commissariat a l' Energie Atomique and G.A.N.I.L. (France) for support enabling this work during a sabbatical. This work was supported by the U.S. Department of Energy under DE-FG02-92ER40714 (IU), DE-FG02-87ER-40316 (WU) and the National Science Foundation under Grant No. PHY-95-28844 (MSU).

-
- [1] U. Brosa and S. Grossman, *Z. Phys. A* **310**, 177 (1983).
 - [2] C.P. Montoya *et al.*, *Phys. Rev. Lett.* **73**, 3070 (1994).
 - [3] A.S. Botvina *et al.*, *Phys. Rev. C* **59**, 3444 (1999).
 - [4] W.U. Schroder *et al.*, *Phys. Rev. Lett.* **44**, 308 (1980).
 - [5] J.D. Bowman, W.J. Swiatecki, and C.-F. Tsang, LBL Report No. LBL-2908 (TID-4500-R61), 1973 (unpublished).
 - [6] J. Gosset *et al.*, *Phys. Rev. C* **16**, 629 (1977).
 - [7] J. Toke *et al.*, *Phys. Rev. Lett.* **75**, 2920 (1995).
 - [8] J. Lukasik *et al.*, *Phys. Rev. C* **55**, 1906 (1997).
 - [9] E. Plagnol *et al.*, *Phys. Rev. C* **61**, 014606 (1999).
 - [10] Y. Larochelle *et al.*, *Phys. Rev. C* **55**, 1869 (1997).
 - [11] S. Piantelli *et al.*, *Phys. Rev. Lett.* **88**, 052701 (2002).
 - [12] M. Colonna *et al.*, *Prog. Part. Nucl. Phys.* **30**, 17 (1993).
 - [13] P.M. Milazzo *et al.*, *Phys. Lett.* **B509**, 204 (2001).
 - [14] P.F. Mastinu *et al.*, *Phys. Rev. Lett.* **76**, 2646 (1996).
 - [15] U. Brosa and S. Grossman, *J. Phys. G: Nucl. Phys.* **10**, 933 (1984).
 - [16] K. Summerer *et al.*, *Phys. Rev. C* **42**, 2546 (1990).
 - [17] B. Davin *et al.*, *Nucl. Instr. Meth.* **A473**, 302 (2001).
 - [18] R.T. de Souza *et al.*, *Nucl. Instr. Meth.* **A295**, 109 (1990).
 - [19] G.D. Westfall *et al.*, *Phys. Rev. Lett.* **37**, 667 (1976).

- [20] F. Bocage, *et al.*, Nucl. Phys. **A676**, 391 (2000).
- [21] G. Casini *et al.*, Phys. Rev. Lett. **71**, 2567 (1993).
- [22] A.A. Stefanini *et al.*, Z. Phys. **A351**, 167 (1995).
- [23] V.E. Viola *et al.*, Phys. Rev. C **31**, 1550 (1985).
- [24] R.J. Charity *et al.*, Nucl. Phys. **A483**, 371 (1988).
- [25] R. Yanez *et al.*, Phys. Rev. Lett. **82**, 3585 (1999).